FEBS Letters 580 (2006) 505–509

Dynamic force spectroscopy of the digoxigenin–antibody complex

G. Neuert*, C. Albrecht, E. Pamir, H.E. Gaub

Lehrstuhl für Angewandte Physik and Center for Nanoscience, Ludwig-Maximilians-Universität, Amalienstrasse 54, 80799 München, Germany

Received 19 October 2005; revised 15 December 2005; accepted 15 December 2005

Available online 27 December 2005

Edited by Peter Brzezinski

Abstract **Small ligands and their receptors are widely used non-covalent couplers in various biotech applications. One prominent example, the digoxigenin–antibody complex, was often used to immobilize samples for single molecule force measurements by optical trap or AFM. Here, we employed dynamic AFM spectroscopy to demonstrate that a single digoxigenin–antibody bond is likely to fail even under moderate loading rates. This effect potentially could lower the yield of measurements or even obscure the unbinding data of the sample by the rupture events of the coupler. Immobilization by multiple antibody–antigen bonds, therefore, is highly recommended. The analysis of our data revealed a pronounced loading rate dependence of the rupture force, which we analyzed based on the well-established Bell–Evans-model with two subsequent unbinding barriers. We could show that the first barrier has a width of $\Delta x_1 = 1.15$ nm and a spontaneous rate of $k_{off1} = 0.015\ s^{-1}$ and the second has a width of $\Delta x_2 = 0.35$ nm and a spontaneous rate of $k_{off2} = 4.56\ s^{-1}$. In the crossover region between the two regimes, we found a marked discrepancy between the predicted bond rupture probability density and the measured rupture force histograms, which we discuss as non-Markovian contribution to the unbinding process.**

Keywords: AFM; Force spectroscopy; Digoxigenin; Antibody; Loading rate; PEG; Nanostructure; Epoxy silane

1. Introduction

Affinity conjugation by means of small ligands and protein receptors has found widespread application for in vitro diagnostics thereby substituting radioactive labeling [1]. Prominent examples like avidin/biotin and digoxigenin–antibody/digoxigenin complexes [1,2] are stable enough to resist dissociation by thermal fluctuations in conventional assays like ELISA. However in biophysical experiments which involve force loading or even forced unbinding of receptor ligand bonds the natural off-rate (k_{off}) is reduced substantially by application of the pulling force. This has first been demonstrated for the forced unbinding of streptavidin/biotin with AFM force spectroscopy [3–7]. These experiments have also proved that low natural off-rates correlate with high unbinding forces [8].

There are many examples, where affinity conjugation was used to investigate the binding properties of receptor–ligand interactions under an applied external force. In one example, it has been exploited for unbinding experiments of double stranded DNA with the optical trap [9]. The DNA-strand was immobilized to a surface bound anti-digoxigenin antibody via a digoxigenin-label [10–18].

In another example, a differential force assay, biotin has been used to immobilize DNA-duplexes to a streptavidin coated silicone stamp. This method is based on the direct comparison of two DNA-duplexes: potential rupture sites assembled in series. Upon application of an external force, one of the duplexes under investigation will break, but not so in the case of the biotin/streptavidin bond, which resists separation up to a higher force regime than the DNA-duplex [19,20].

Due to the lowering of the natural off-rate under force, it is probable that affinity conjugation systems, which are stable in conventional assays, may fail in experiments under force load. This could lead to low yield measurements or more seriously to artifacts, when rupture events of the coupler complexes instead of the sample are traced in receptor/ligand studies. Hence, the affinity conjugation pair has to be chosen carefully depending on the loading rates realized in the experiment.

In this study, we have investigated the rupture probability of the digoxigenin/anti-digoxigenin complex over a wide range of loading rates with the intention of estimating its stability for biophysical experiments under force load.

A fundamental model for forced unbinding of receptor–ligand pairs was proposed by Bell and later investigated in detail by Evans [21,22]. Here, the binding potential is characterized by the potential depth and the potential width. While the potential width (Δx) is only accessible by forced unbinding experiments, the potential depth, which correlates with the natural off-rate, can be deduced from ensemble measurements as well [23]. In contrast to the potential width, which is assumed to be constant in this model, the potential depth is lowered if a force is applied to the complex. It has been demonstrated that the Bell model predicts the rupture probability of a complex in dependence of the applied loading rate. However, whether this is also true or not for the high loading range has thus far not been investigated comprehensively.

In a first approach, we analyzed our data due to the conventional assumption that Δx is constant over the whole range of loading rates. In this way, we are able to show, that interpolation of our data from the low loading range results in a natural dissociation rate $k_{off1} = 0.015\ s^{-1}$, which is in good agreement with bulk measurements on Fv-fragments [24]. Here, we are near equilibrium and therefore a constant Δx is reasonable.

For the high loading rate, however, we found a marked discrepancy between our data and the approximation of Δx = constant, which we will discuss at the end of the article.

*Corresponding author. Fax: +49 89 2180 2050.
E-mail address: gregor.neuert@physik.uni-muenchen.de (G. Neuert).

0014-5793/$32.00
doi:10.1016/j.febslet.2005.12.052

2. Material and methods

2.1. Slide preparation

Commercial epoxy functionalized slides (Schott, Nexterion, Mainz, Germany) were used for covalent coupling of di-amino-polyethyleneglycol (di-NH_2-PEG, MW 6000 g/mol, Rapp Polymere, Freiburg, Germany). An amount of 75 mg of di-NH_2-PEG was homogeneously distributed over the whole epoxy slide and heated at 95 °C for 15 min until melting. To obtain a thin PEG layer, a second epoxy slide was placed up side down onto the first one. This "sandwich" was heated at 95 °C for 24 h. After carefully separating the slides, they were rinsed with Millipore water several times to wash away the unbound di-NH_2-PEG and dried afterwards with N_2 [25].

The NH_2 functional PEG surface was then converted into a COOH surface by covering the surface with a 200 µl solution of 2 g/ml glutaric anhydride ($C_5H_6O_3$, Aldrich) in *N*,*N*-dimethylformamide (DMF, $HCON(CH_3)_2$, Aldrich). A second NH_2 functional PEG slide was placed onto the slide to cover it completely with glutaric anhydride. This sandwich was incubated at room temperature for 12 h in a DMF atmosphere. After incubation, the slides were washed with DMF, Millipore water and finally dried in the oven. The PEG slides with the COOH functionalized surface were stored in an Ar-atmosphere until activation.

2.2. Cantilever preparation

The cantilevers (Bio-lever, Olympus, Tokyo, Japan) were cleaned in sulfuric acid (H_2SO_4, 95%, Fluka, Germany) containing 17 mg/ml potassium dichromate ($K_2Cr_2O_7$, Sigma, Germany) for 10 min, then washed in Millipore water and dried. Silanization was achieved by keeping the cantilevers in concentrated 3-glycidoxypropyl-trimethoxysilane (Sigma, München, Germany) for 1–2 min. Afterwards, they were washed with toluol (Sigma, München, Germany) and Millipore water and heated at 95 °C for 30 min, which finally resulted in epoxy functionalized tips [26]. The PEG melting described previously was also applied to the epoxy functionalized cantilevers.

For each cantilever, 50 mg of di-NH_2-PEG were put in adequate holes of a Teflon block and heated until melting. Now the cantilevers were placed carefully in the liquid di-NH_2-PEG drops and heated at 95 °C for 12 h. Finally, the cantilevers were washed several times in hot Millipore water and subsequently dried in the oven. As a result of this procedure, the cantilever tips became passivated and amino-functional.

2.3. Anti-digoxigenin antibody and digoxigenin coupling

The activation of COOH groups on the PEG glass slide was performed with 1-ethyl-3-(3-dimethylaminopropyl) carbodiimide hydrochloride (EDC, Sigma) and 3-*O*-methylcarbonyl-aminocaproic acid–*N*-hydroxysuccinimide ester (NHS). For each slide, 200 µl of a 1:1 solution of 100 mM EDC and 100 mM NHS in Millipore water were put onto the slide and covered with a thin glass cover slide. The slide was incubated for 30 min in an H_2O-atmosphere, afterwards washed with Millipore water and dried in a stream of N_2. Monoclonal anti-digoxigenin antibody from mouse (IgG1, clone 1.71.256, Roche, Germany) with a concentration of 100 µg/ml (in 10 mM potassium phosphate buffer, 75 mM NaCl, 5% raffinose, 0.01% 2-methyl-isothiazolone (MIT), pH 7.8) was spotted onto the pre-activated COOH surface and then incubated for 1 h in H_2O-atmosphere to allow for the reaction of the amino groups of the antibody with the pre-activated COOH groups forming a covalent bond. Finally, the slide was washed with PBS (phosphate buffered saline, pH 7.4) to remove non-covalently attached antibodies and then stored in PBS at 4 °C until use.

The cantilever tips were incubated for 1 h in 20 µl drops of the digoxigenin-3-*O*-methylcarbonyl-aminocaproic acid–*N*-hydroxysuccinimide ester solution (10 mM digoxigenin–NHS solved in sodium borate, 100 mM, pH 8.5), to allow for a covalent reaction with the NH_2 groups of the PEG spacer. Finally, the cantilevers were washed with Millipore water to remove non-covalently attached digoxigenin–NHS and stored in Millipore water at 4 °C until use (see Fig. 1).

2.4. Dynamic force spectroscopy

All AFM measurements were performed at room temperature in PBS with a homebuilt instrument [27]. Cantilevers with spring constants of 6 and 8.08 pN/nm (A-Bio-Lever), and 50 pN/nm (B-Bio-Lever) were used. The spring constants were measured in each experiment as described previously [28,29]. During the experiment the retract velocity was held constant, whereas the contact time and the approach velocity were adjusted in order to obtain single binding events. When non-specific or multiple binding events occurred, the approach velocity was increased and/or the contact time was decreased in order to reduce those effects. In the case of infrequent specific binding events the parameters were adjusted vice versa. Typically the approach velocity was on the order of magnitude of the retract velocity and the contact time varied from 0 to 5 s.

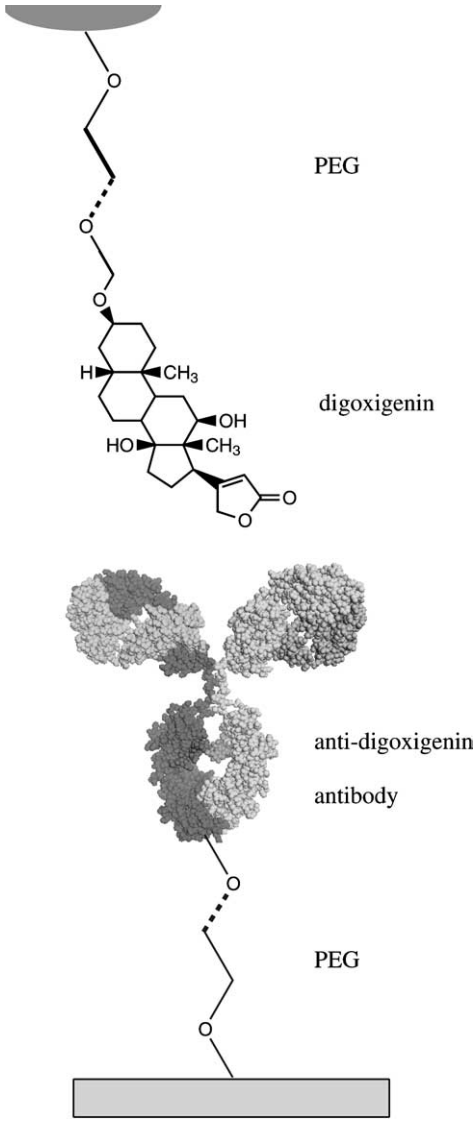

Fig. 1. Schematic view of AFM-tip, PEG spacer, digoxigenin, anti-digoxigenin antibody and slide.

Several hundreds of approach and retract cycles were carried out to provide appropriate statistical significance. For each experiment, a broad distribution of loading rates was obtained by varying the retract velocities between 20 nm/s and 20 µm/s [4].

2.5. Data extraction

The recorded cantilever deflection traces were converted into force against extension curves (Fig. 2). Each experiment consisted of several hundreds of force distance curves measured at one constant retract velocity. These curves were analyzed all together to obtain both, the rupture force (the force at which the antigen–antibody bond breaks) and the loading rate dF/dt. The loading rate describes how much force was applied to the bond at a certain time shortly before the rupture

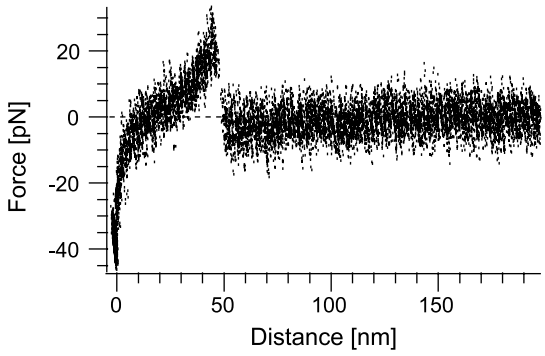

Fig. 2. Force against distance curve. The values of the rupture force, the rupture length and the loading rate were obtained from these curves as described in the text.

event occurs. The rupture force was determined as described previously [30,31]. The loading rate was determined with a line-fit of the force curve prior to rupture, according to previous studies [30,31].

2.6. Data analysis

Rupture forces and appropriate loading rates were then plotted in two histograms for each experiment with the same retract velocity.

These histograms were analyzed in a two-step procedure. In the first step, the force and the loading rate histograms with the same retract velocity were fitted with a Gaussian distribution to find the maximum of the histograms. This was done for all measured histograms of the different experiments with retract velocities between 20 nm/s and 20 μm/s. The maximum values of the Gaussian fits were plotted in a force vs. logarithmic loading rate diagram.

The maximum obtained from the force histogram represents the most probable rupture force F^*

$$F^* = \frac{k_B T}{\Delta x} \ln \frac{\dot{F} \Delta x}{k_B T \cdot k_{off}} \quad (1)$$

with k_B is Boltzmann constant, T is the temperature, k_{off} is the natural dissociation rate at zero force, Δx is the potential width between the bound and the transition state and $\dot{F} = dF/dt$, the loading rate. A linear fit of the force vs. logarithm of the loading rate according to Eq. (1) reveals the natural dissociation rate at zero force k_{off} and the potential width Δx for the digoxigenin/anti-digoxigenin complex.

In the second step, the force histogram was normalized to be comparable with the probability density function $p(F)$ containing k_{off} and Δx [4,30–32]

$$p(F) = k_{off} \exp\left(\frac{F\Delta x}{k_B T}\right) \frac{1}{\dot{F}} \exp\left(-k_{off} \int_0^F dF' \exp\left(\frac{F\Delta x}{k_B T}\right) \frac{1}{\dot{F}}\right). \quad (2)$$

3. Results and discussion

In this study we determined the energy landscape of the digoxigenin–antibody complex in order to assess its properties as a coupler for samples in dynamic force spectroscopy.

Rupture forces were extracted from force curves in a range of 30 up to 63 000 pN/s. The maximum of the rupture force histograms was plotted against the corresponding loading rate dF/dt (Fig. 3) in order to extract k_{off} and Δx. The diagram shows a non-linear dependence of the force as a function of the logarithm of the loading rate. This diagram was therefore fitted with two lines. The line-fit for low loading rates (Fig. 3, dashed line) reveals a dissociation rate at zero force of $k_{off1} = 0.015\ s^{-1}$ and a potential width of $\Delta x_1 = 1.15$ nm. This natural dissociation rate corresponds very well to the literature

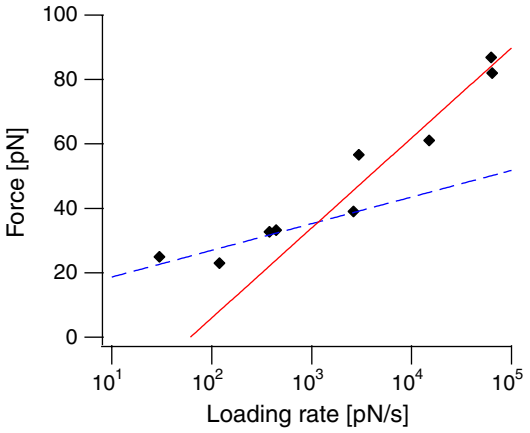

Fig. 3. Most probable rupture force F^* plotted against the logarithm of the loading rate. Each point in the diagram represents the most probable rupture force F^* and the related most probable loading rate dF/dt. The maximum was determined by a Gaussian fit to the force and the loading rate histogram at a constant retraction speed (black diamonds). Two distinct regions are observed and fitted with two line-fits according to Eq. (1). The low loading rate region can be described with $\Delta x_1 = 1.15$ nm and $k_{off1} = 0.015\ s^{-1}$ (dashed line) and the high loading rate region can be described with $\Delta x_2 = 0.35$ nm and $k_{off2} = 4.56\ s^{-1}$ (solid line).

value of $k_{off} = 0.023\ s^{-1}$ received from bulk measurements of comparable anti-digoxigenin Fv-fragments [24]. At high loading rates a $k_{off2} = 4.56\ s^{-1}$ and $\Delta x_2 = 0.35$ nm was deduced (Fig. 3, solid line). According to Merkel [4], who investigated the unbinding of biotin/streptavidin, the two regions correspond to two barriers in the energy landscape of the complex. Given that these values represent the energy landscape of the anti-digoxigenin/digoxigenin interaction, it should be possible to extract similar k_{off} and Δx values directly from the force histogram [31,32]. Therefore, the probability density function $p(F)$ of Eq. (2) should fit the observed force histograms.

In order to test this assumption, we fitted the probability density function $p(F)$ to the observed normalized last rupture force histogram as shown in Fig. 4. The histogram in Fig. 4a was measured at a loading rate of 120 pN/s and can be fitted with the calculated probability density function $p(F)$ using $k_{off1} = 0.015\ s^{-1}$ and $\Delta x_1 = 1.15$ nm (dashed line). For high loading rates, the measured force histogram (loading rate of 14 950 pN/s) can also be fitted with the probability density function $p(F)$ using $k_{off2} = 4.56\ s^{-1}$ and $\Delta x_2 = 0.35$ nm as shown in Fig. 4b (solid line). These two histograms at different loading rates describe the two regions in good accordance and the k_{off} and Δx values are in the same range as seen in previous studies (k_{off}: 10^{-3}–$10^2\ s^{-1}$ and Δx: 0.4–1.0 nm) [23,33,34].

The practical implication of the above findings for experiments under force load can be illustrated by the following Gedankenexperiment: A receptor–ligand complex under investigation was immobilized by the digoxigenin–antibody complex. At a low loading rate of 120 pN/s the maximum of the rupture force of digoxigenin/anti-digoxigenin is 24 pN as shown in Fig. 4a. At a given rupture force of the complex under investigation of 10 pN, the probability for bond breakage of digoxigenin/anti-digoxigenin is still 10% compared to 100% probability at 24 pN (dashed line in Fig. 4a). Consequently the measurement of a force of 10 pN in a setup that uses the digoxigenin/anti-digoxigenin system as affinity conjugation under

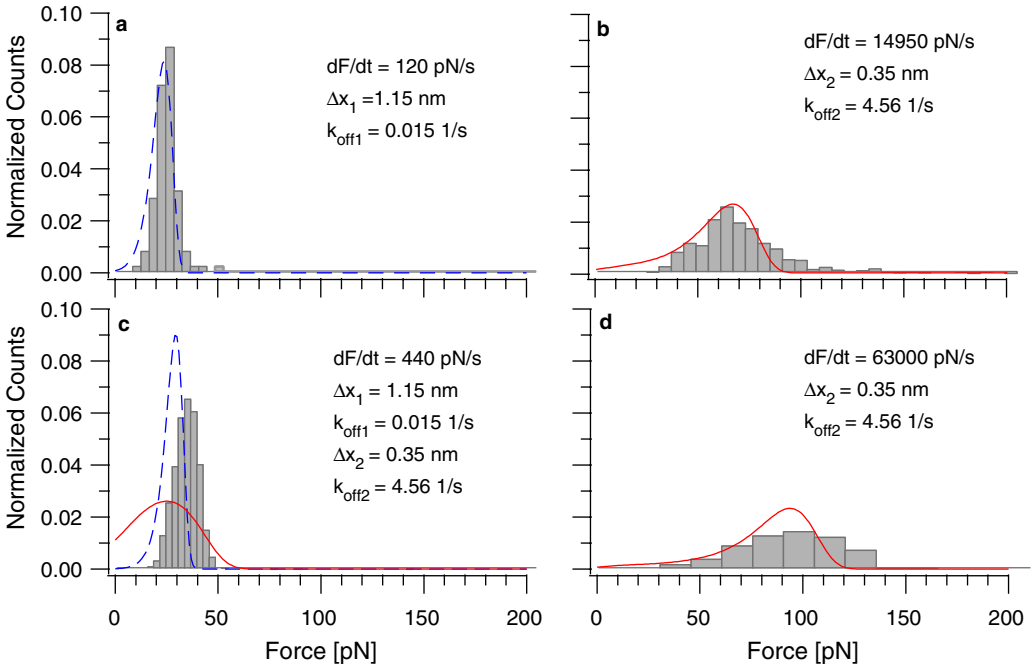

Fig. 4. Force histograms at different loading rates dF/dt. Rupture forces are plotted in histograms (bars: a, 85 curves; b, 644 curves; c, 925 curves; d, 155 curves) and compared with the calculated probability density function $p(F)$ (dashed line with $\Delta x_1 = 1.15$ nm, $k_{off1} = 0.015\ s^{-1}$, solid line with $\Delta x_2 = 0.35$ nm, $k_{off2} = 4.56\ s^{-1}$).

the above conditions, results in a 10% rupture probability of the affinity conjugation complex and a 90% rupture probability of the system under investigation.

Rupture of the digoxigenin–antibody coupler might lead to low yields of force curves during the measurement or to a misinterpretation of the unbinding of receptor and ligand. Therefore it is highly recommended to make use of avidity effects by using multiple complexes for immobilization instead of single bonds [9,12,17,35].

The fit of the data shown in Fig. 3 results in two different pairs of values for k_{off} and Δx. With these values, we are able to fit force histograms as illustrated in Fig. 4a and b above. However, we also tried to apply this analysis to the force histograms at very high loading rates and to the interception between the two line-fits as seen in Fig. 3. For a loading rate of 63 000 pN/s the measured force histogram (Fig. 4d) is broader compared to the calculated probability density function (solid line). These differences are dramatic, because the shape of the probability density function $p(F)$ depends heavily on the natural dissociation rate at zero force k_{off} and the potential width Δx. For a good match of the measured force histogram and the calculated probability function $p(F)$ completely different values for k_{off} and Δx would have to be used.

The other section of interest is near the interception of the two line-fits in Fig. 3. The force histogram shown in Fig. 4c was measured at a loading rate of 440 pN/s and compared to two plausible probability density functions. The first probability density function uses the k_{off1} and Δx_1 values observed at low loading rates (dashed line) and the second probability density function uses the k_{off2} and Δx_2 values observed at high loading rates (solid line). It is clear that both probability density functions do not fit the observed force histogram. Only by once again using completely different values for k_{off} and Δx, the experimental force histogram can be fitted adequately. Therefore we conclude, that the analysis based on the assumption of two barriers in the energy landscape of the receptor ligand pair [4,30], can potentially be misleading. In particular at the intermediate regime, large deviations occur between the measured data and the obtained fits. This indicates that perhaps the underlying dissociation mechanism might deviate from the simplistic two-barrier model at this region.

One reason for the misleading analysis might be the assumption made in this model, that the energy wells are deep and the distance Δx between the minima and the transition state are fixed during the applied load [4,21,30,36,37]. While this approximation was again confirmed by the close correlation of k_{off1} deduced from the low loading rate range with k_{off} from affinity sensor measurements, it obviously fails for higher forces. Because, in this study, we applied large external forces, which may alter the energy landscape of the complex dramatically, the assumption of a Markovian like behavior of two distinct states may not hold true anymore.

Kramer's theory could be an alternative to overcome the problem, since the binding width is not assumed to be constant in this model [38]. To give a full description of the measured force histogram, further theoretical investigations are needed.

Acknowledgments: We thank Thomas Nicolaus for technical assistance in preparing the surfaces and Julia Sedlmair, Julia Morfill, Kerstin Blank and Kay Gottschalk for their helpful discussions. This work was supported by the Deutsche Forschungsgemeinschaft.

References

[1] Hermanson, G. (1996) Bioconjugate Techniques, Academic Press, London.

[2] Kessler, C., Holtke, H.J., Seibl, R., Burg, J. and Muhlegger, K. (1990) Non-radioactive labeling and detection of nucleic acids. I. A novel DNA labeling and detection system based on digoxigenin: anti-digoxigenin ELISA principle (digoxigenin system). Biol. Chem. Hoppe Seyler 371, 917–927.
[3] Grubmüller, H., Heymann, B. and Tavan, P. (1996) Ligand binding: molecular mechanics calculation of the streptavidin biotin rupture force. Science 271, 997–999.
[4] Merkel, R., Nassoy, P., Leung, A., Ritchie, K. and Evans, E. (1999) Energy landscapes of receptor–ligand bonds explored with dynamic force spectroscopy. Nature 397, 50–53.
[5] Florin, E.L., Rief, M., Lehmann, H., Ludwig, M., Dornmair, C., Moy, V.T. and Gaub, H.E. (1995) Sensing specific molecular-interactions with the atomic-force microscope. Biosens. Bioelectron. 10, 895–901.
[6] Izrailev, S., Stepaniants, S., Balsera, M., Oono, Y. and Schulten, K. (1997) Molecular dynamics study of unbinding of the avidin–biotin complex. Biophys. J. 72, 1568–1581.
[7] Lee, G.U., Kidwell, D.A. and Colton, R.J. (1994) Sensing discrete streptavidin–biotin interaction with atomic force microscopy. Langmuir 10, 354–357.
[8] Moy, V.T., Florin, E.L. and Gaub, H.E. (1994) Intermolecular forces and energies between ligands and receptors. Science 266, 257–259.
[9] Lang, M.J., Fordyce, P.M., Engh, A.M., Neuman, K.C. and Block, S.M. (2004) Simultaneous, coincident optical trapping and single-molecule fluorescence. Nat. Methods 1, 133–139.
[10] Bockelmann, U. (2004) Single-molecule manipulation of nucleic acids. Curr. Opin. Struct. Biol. 14, 368–373.
[11] Allemand, J.F., Bensimon, D. and Croquette, V. (2003) Stretching DNA and RNA to probe their interactions with proteins. Curr. Opin. Struct. Biol. 13, 266–274.
[12] Bryant, Z., Stone, M.D., Gore, J., Smith, S.B., Cozzarelli, N.R. and Bustamante, C. (2003) Structural transitions and elasticity from torque measurements on DNA. Nature 424, 338–341.
[13] Liphardt, J., Onoa, B., Smith, S.B., Tinoco, I. and Bustamante, C. (2001) Reversible unfolding of single RNA molecules by mechanical force. Science 292, 733–737.
[14] Ha, T. (2001) Single-molecule fluorescence methods for the study of nucleic acids. Curr. Opin. Struct. Biol. 11, 287–292.
[15] Quake, S.R., Babcock, H. and Chu, S. (1997) The dynamics of partially extended single molecules of DNA. Nature 388, 151–154.
[16] Shaevitz, J.W., Abbondanzieri, E.A., Landick, R. and Block, S.M. (2003) Backtracking by single RNA polymerase molecules observed at near-base-pair resolution. Nature 426, 684–687.
[17] Koch, S.J., Shundrovsky, A., Jantzen, B.C. and Wang, M.D. (2002) Probing protein–DNA interactions by unzipping a single DNA double helix. Biophys. J. 83, 1098–1105.
[18] Williams, M.C. and Rouzina, I. (2002) Force spectroscopy of single DNA and RNA molecules. Curr. Opin. Struct. Biol. 12, 330–336.
[19] Albrecht, C. et al. (2003) DNA: a programmable force sensor. Science 301, 367–370.
[20] Blank, K. et al. (2003) A force-based protein biochip. Proc. Natl. Acad. Sci. USA 100, 11356–11360.
[21] Bell, G.I. (1978) Models for the specific adhesion of cells to cells. Science 200, 618–627.
[22] Evans, E. and Ritchie, K. (1997) Dynamic strength of molecular adhesion bonds. Biophys. J. 72, 1541–1555.
[23] Schwesinger, F. et al. (2000) Unbinding forces of single antibody–antigen complexes correlate with their thermal dissociation rates. Proc. Natl. Acad. Sci. USA 97, 9972–9977.
[24] Chen, G., Dubrawsky, I., Mendez, P., Georgiou, G. and Iverson, B.L. (1999) In vitro scanning saturation mutagenesis of all the specificity determining residues in an antibody binding site. Protein Eng. 12, 349–356.
[25] Piehler, J., Brecht, A., Valiokas, R., Liedberg, B. and Gauglitz, G. (2000) A high-density poly(ethylene glycol) polymer brush for immobilization on glass-type surfaces. Biosens. Bioelectron. 15, 473–481.
[26] Hugel, T., Grosholz, M., Clausen-Schaumann, H., Pfau, A., Gaub, H. and Seitz, M. (2001) Elasticity of single polyelectrolyte chains and their desorption from solid supports studied by AFM based single molecule force spectroscopy. Macromolecules 34, 1039–1047.
[27] Holland, N.B. et al. (2003) Single molecule force spectroscopy of azobenzene polymers: switching elasticity of single photochromic macromolecules. Macromolecules 36, 2015–2023.
[28] Butt, H.J. and Jaschke, M. (1995) Calculation of thermal noise in atomic-force microscopy. Nanotechnology 6, 1–7.
[29] Hugel, T. and Seitz, M. (2001) The study of molecular interactions by AFM force spectroscopy. Macromol. Rapid Commun. 22, 989–1016.
[30] Evans, E. and Ritchie, K. (1999) Strength of a weak bond connecting flexible polymer chains. Biophys. J. 76, 2439–2447.
[31] Friedsam, C., Wehle, A.K., Kühner, F. and Gaub, H.E. (2003) Dynamic single-molecule force spectroscopy: bond rupture analysis with variable spacer length. J. Phys. Condens. Mat. 15, S1709–S1723.
[32] Kühner, F., Costa, L.T., Bisch, P.M., Thalhammer, S., Heckl, W.M. and Gaub, H.E. (2004) LexA–DNA bond strength by single molecule force spectroscopy. Biophys. J. 87, 2683–2690.
[33] Berquand, A., Xia, N., Castner, D.G., Clare, B.H., Abbott, N.L., Dupres, V., Adriaensen, Y. and Dufrene, Y.F. (2005) Antigen binding forces of single antilysozyme Fv fragments explored by atomic force microscopy. Langmuir 21, 5517–5523.
[34] Strigl, M., Simson, D.A., Kacher, C.M. and Merkel, R. (1999) Force-induced dissociation of single protein A–IgG bonds. Langmuir 15, 7316–7324.
[35] Brower-Toland, B.D., Smith, C.L., Yeh, R.C., Lis, J.T., Peterson, C.L. and Wang, M.D. (2002) Mechanical disruption of individual nucleosomes reveals a reversible multistage release of DNA. Proc. Natl. Acad. Sci. USA 99, 1960–1965.
[36] Evans, E. (2001) Probing the relation between force–lifetime and chemistry in single molecular bonds. Annu. Rev. Biophys. Biomol. Struct. 30, 105–128.
[37] Hänggi, P. and Talkner, P. (1990) Reaction-rate theory: fifty years after Kramers. Rev. Mod. Phys. 62, 251–341.
[38] Kramers, H.A. (1940) Physica 7, 284.